The FEBS Journal

FEBS PRESS science publishing by scientists

Formation of adenovirus DNA replication compartments and viral DNA accumulation sites by host chromatin regulatory proteins including NPM1

Michelle Jane Genoveso[1,2], Miharu Hisaoka[2], Tetsuro Komatsu[3,4], Harald Wodrich[3], Kyosuke Nagata[2] and Mitsuru Okuwaki[2,5]

1 Ph.D. Program in Humanics, School of Integrative and Global Majors, University of Tsukuba, Japan
2 Faculty of Medicine, University of Tsukuba, Japan
3 CNRS UMR 5234, Fundamental Microbiology and Pathogenicity, Université de Bordeaux, France
4 Division of Transcriptomics, Medical Institute of Bioregulation, Kyushu University, Fukuoka, Japan
5 School of Pharmacy, Kitasato University, Tokyo, Japan

Keywords
adenovirus; chromatin; NPM1; nucleolus; ViPR body

Correspondence
M. Okuwaki, School of Pharmacy, Kitasato University, 5-9-1 Shirokane, Minato-ku, Tokyo 108-8641, Japan
Tel: +81 3 5791 6245
E-mail: okuwakim@pharm.kitasato-u.ac.jp

(Received 8 March 2019, revised 19 June 2019, accepted 29 July 2019)

doi:10.1111/febs.15027

The adenovirus (Ad) genome is believed to be packaged into the virion by forming a chromatin-like structure. The replicated viral genome is likely to be condensed through binding with viral core proteins before encapsidation. Replicated viral genomes accumulate in the central region of the nucleus, which we termed virus-induced postreplication (ViPR) body. However, the molecular mechanism by which the nuclear structure is reorganized and its functional significance in virus production are currently not understood. In this study, we found that viral packaging protein IVa2, but not capsid proteins, accumulated in the ViPR body. In addition, nucleolar chromatin regulatory proteins, nucleophosmin 1 (NPM1), upstream binding factor, and nucleolin accumulated in the ViPR body in late-stage Ad infection. NPM1 depletion increased the nuclease-resistant viral genome and delayed the ViPR body formation. These results suggested that structural changes in the infected cell nucleus depend on the formation of viral chromatin by host chromatin regulatory proteins. Because NPM1 depletion decreases production of the infectious virion, we propose that host factor-mediated viral chromatin remodeling and concomitant ViPR body formation are prerequisites for efficient encapsidation of Ad chromatin.

Introduction

Despite causing several types of human infections, human adenovirus (Ad) has been developed as a very efficient gene delivery and therapy tool [1]. It is crucial to understand the molecular mechanisms by which viral DNA is replicated, viral genes expressed, capsids assembled, and the viral genome packaged into the virion. However, the late stages (i.e., genome/chromatin remodeling, packaging, and capsid assembly) are yet to be fully elucidated.

The Ad particle is nonenveloped and comprises an icosahedral protein shell (60–100 nm in diameter) surrounding a protein core that contains the linear, double-stranded DNA genome of ~ 36 000 base pairs. The protein shell is comprised of major capsid proteins

Abbreviations
Ad, adenovirus; DBP, DNA-binding protein; DMEM, Dulbecco's modified Eagle's medium; LLPS, liquid–liquid phase separation; MOI, multiplicity of infection; NCL, nucleolin; NPM1, nucleophosmin 1; PCV, packed cell volume; qPCR, quantitative polymerase chain reaction; RSB, reticulocyte standard buffer; TAF-I, template activating factor-I; UBF, upstream binding factor; ViPR body, virus-induced postreplication body.

hexon (protein II), penton base (protein III), fiber (protein IV), and minor capsid proteins IIIa, VI, VIII, and IX. Four proteins [i.e., protein V, protein VII, μ, and terminal protein (TP)] condense the Ad genome in the viral core, forming a chromatin-like organization [2–4]. The proteins IVa2, L4 33K, L4 22K, E2 72K, and L1 52/55K are involved in capsid assembly and/or genome packaging [5–12].

Two distinct capsid assembly and genome-packaging models have been proposed, sequential and concomitant. In the sequential model, the replicated genome is incorporated into preformed capsids. In the concomitant model, viral capsids are assembled on the replicated viral genome. In a previous study, we used pulse-chase experiments to demonstrate that replicated DNA accumulates in the sites termed 'virus-induced postreplication (ViPR) body', which is formed inside the viral genome replication compartments in late-stage Ad infection [13]. Although the function of the ViPR body is unknown, it is speculated that replicated viral genome packaged in viral-specific chromatin structure is maintained in the ViPR body for efficient encapsidation, because viral capsid assembly and genome packaging have been suggested to occur outside the viral replication compartments [14].

Various host proteins are involved in the Ad lifecycle. Of these, we have identified NPM1 (nucleophosmin, B23, numatrin), an acidic nucleolar protein, as a stimulatory factor for *in vitro* replication of Ad DNA complexed with viral basic proteins. NPM1 has histone chaperone, DNA and RNA binding, and ribonuclease activities [15–18], and plays various roles in cellular processes such as ribosome biogenesis and centrosome duplication [19,20]. NPM1 also functions as a viral core protein pre-VII chaperone and suppresses the formation of aggregates between DNA and core proteins *in vitro* [21]. Consistent with this biochemical activity, NPM1 depletion significantly increases the association of viral core proteins V and VII, and cellular histones with viral DNA in infected cells [22]. Importantly, NPM1 depletion impedes the production of infectious progeny virions without affecting Ad genome replication and transcription [22]. These results indicate that NPM1 is involved in the Ad infection cycle at a step downstream of viral genome replication. In addition, NPM1 interacts with the empty Ad particle, suggesting a putative role in capsid assembly [23]. Interestingly, NPM1 is reported to be involved in the core and capsid assembly of DNA viruses, such as hepatitis B virus [24] and human papilloma 16 virus [25]. Notwithstanding these findings, the function of NPM1 in late-stage Ad infection remains to be fully understood.

Template-activating factor-I (TAF-I), an acidic histone chaperone, binds to the viral genome complexed with viral core proteins through the interaction with core protein VII, especially in early-stage Ad infection [26]. The TAF-I-Ad genome interaction is required for efficient transcription and expression of early gene transcription. In addition, the nucleolar proteins nucleolin (NCL), upstream binding factor (UBF), and Mybbp1a [13,27,28] are involved in the Ad infection cycle, although their exact functions remain to be determined.

In this study, we examined the structural reorganization of the cell nucleus during the Ad infection cycle by focusing on the localization of viral DNA replication, genome packaging, and virus capsid proteins. Further analyses suggested that the host chromatin regulatory proteins NPM1, NCL, and UBF are involved in the regulation of the infected cell nuclear structure in late-stage Ad infection by accumulating in the ViPR body. These results will contribute to our understanding how the Ad genome is produced and packaged into the virions in late-stage Ad infection.

Results

Subnuclear structures in late-stage Ad infection

Nuclear structures, including viral replication compartments, significantly change in late-stage Ad infection [13,29]. To confirm these changes and reveal newly formed subnuclear structures upon Ad infection, we performed indirect immunofluorescence assay with U2OS cells infected with human Ad type 5 (HAdV5) using an antibody against the viral single-stranded DNA-binding protein (DBP) required for viral DNA replication. Using the antibody against DBP enabled us to visualize nuclear territories where Ad DNA replication took place [30]. As previously reported, we found that DBP exhibits several localization patterns in Ad-infected cells at different time points postinfection, while we detected no DBP expression in uninfected cells (Fig. 1A,B). At 12 h postinfection (hpi), in the majority of cells, DBP showed numerous dots or foci spread throughout the nucleus. At 18 hpi, we observed the formation of DBP ring-like structures (classical replication compartments) in most cells; at 24 hpi, these ring-like structures increased in size and became disrupted or discontinuous (late replication compartments). At a closer look, the disrupted DBP rings were comprised of dots, which were adjacent but not connected to each other, hence making the ring looked discontinuous. In addition, the staining for cellular DNA did not significantly change until DBP

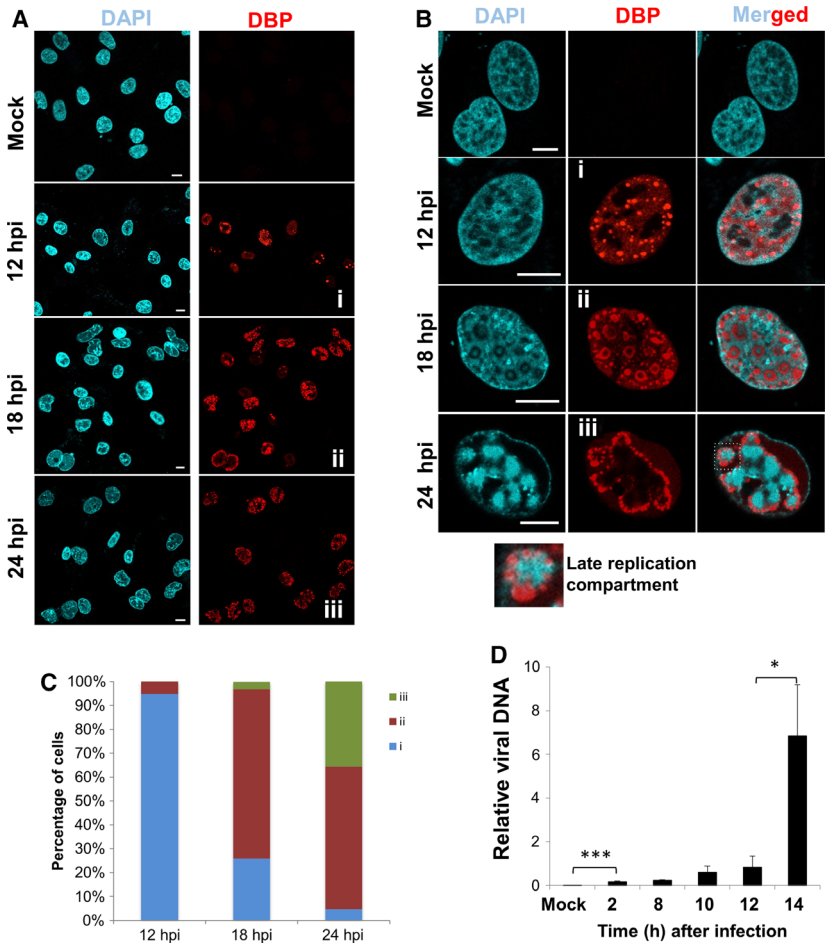

Fig. 1. Subnuclear structures in late-stage Ad infection. (A–C) DBP localization patterns. U2OS cells were either mock infected or infected with HAdV5 and subjected to immunofluorescence (IF) analyses at 12, 18, and 24 h postinfection (hpi). DNA was stained with DAPI. Merged images are shown in the 3rd column in B. Images were obtained with 20× and 63× objective lenses for A and B, respectively. Higher magnified images of the region marked by square in B is shown at the bottom of the panel as representative for the late replication compartment. The most representative localization patterns at each time point were picked up and shown. Based on the localization patterns of DBP and DNA, the localization patterns were categorized into three patterns; pattern i shows that small DBP foci are formed and DNA staining pattern is similar to that of mock infected cells; pattern ii shows that DBP rings are formed and DNA is excluded from the DBP rings; pattern iii shows DBP ring disintegrates and DNA accumulates inside the disrupted DBP rings. The numbers of the cells showing the localization patterns i to iii at each time point were quantified and the data were graphically shown in panel C (n = 155, 182, and 194 for 12, 18 and 24 hpi, respectively). (D) Quantitative analyses of Ad genomic DNA. U2OS cells were mock- or HAdV5-infected with MOI of 20. At 2, 8, 10, 12, and 14 hpi, DNA was purified from the cells and the amounts of viral DNA were examined by qPCR using a primer set specific for the *VA RNA1* region. The amount of viral DNA at 2 hpi was set to 1.0 and the relative amounts of Ad DNA were quantified. The amounts of viral DNA were normalized to that of the *ribosome RNA* genes. The data were the average of three independent experiments with duplicate PCR reactions and error bars indicating ±SD. *P*-values were calculated using student's *t*-test (*$P < 0.05$; ***$P < 0.001$). Scale bars, 10 μm.

showed a dot-like localization pattern. When DBP formed ring-like structures, DNA was excluded from the DBP rings and was also detected inside them. Furthermore, when the DBP rings disintegrated, DNA clearly accumulated in distinct structures in the central region of the infected cell nucleus, the ViPR body [13]. We categorized these localization patterns into three types (i–iii) on the basis of DBP and DNA localization patterns, showed typical localization patterns at each time point (Fig. 1B), and quantified their appearance over time (Fig. 1C). The categorization was in good agreement with a previous one that we detected with the cellular protein USP7 [13]. These results suggested that in late-stage Ad infection, DBP first accumulates in numerous dots and then classical DNA replication compartments (DBP ring) (pattern ii) were formed,

followed by disintegration or transformation to form late replication compartments (pattern iii). Importantly, since viral DNA detected by quantitative polymerase chain reaction (qPCR) started to increase during 8–12 hpi (Fig. 1D), viral DNA replication was likely to initiate in pattern i cells. DNA accumulation clearly increased at 14 hpi with an increase in pattern ii and iii cells (during 12 and 18 hpi). Since the ViPR body showed low cellular histones and high core protein VII densities [13,29], the accumulated DNA is likely to be replicated viral DNA. Our previous results with an *in vivo*-tagging system [29] support this notion. Cellular DNA could be detected at the nuclear periphery and around ViPR bodies showing distinct DNA intensities. In addition, we cannot exclude the possibility that a minor population of cellular DNA was also accumulated to ViPR bodies.

Putative sites of Ad genome packaging and capsid assembly

To gain insight into subnuclear territories where infectious Ad virion assembly occurs relative to ViPR body sites, we examined the localization of Ad packaging protein IVa2 and capsid proteins pVI and pIX. Since the localization of pVI is similar to that of the major capsid protein Hexon (data not shown) and several studies have reported the role of IVa2 in Ad packaging through its binding to the packaging sequence [8,31,32], examining the pVI, pIX, and IVa2 localization allows us to suppose the sites of capsid assembly and genome packaging. Indirect immunofluorescence assay revealed a dispersed IVa2 signal throughout the nucleus and cytoplasm at 12 hpi (Fig. 2A). IVa2 started to accumulate in the nucleus but not in Ad DNA replication sites where DBP rings were formed. IVa2 was excluded from DBP rings (classical replication compartments, see enlarged panel at the bottom of Fig. 2A). Interestingly, IVa2 formed irregular ring-like structures inside the DBP dots and at the periphery of the ViPR body when late replication compartments were formed (pattern iii, see also Fig. 2B). In addition, IVa2 was also detected at sites where DNA was excluded (DNA-free regions shown by arrowheads in Fig. 2B) and clearly colocalized with the capsid protein pVI (Fig. 2B). Similarly, we also detected the minor capsid protein pIX in the DNA-free region as did pVI, although pIX was also detected in small dots in pattern ii cells, which did not overlap with the replication compartments marked by DBP (Fig. 2C). The dot-like localization of pIX could be explained by its additional roles in the Ad life cycle, aside from being a minor component of the capsid, such as transcriptional activation and nuclear protein reorganization for an

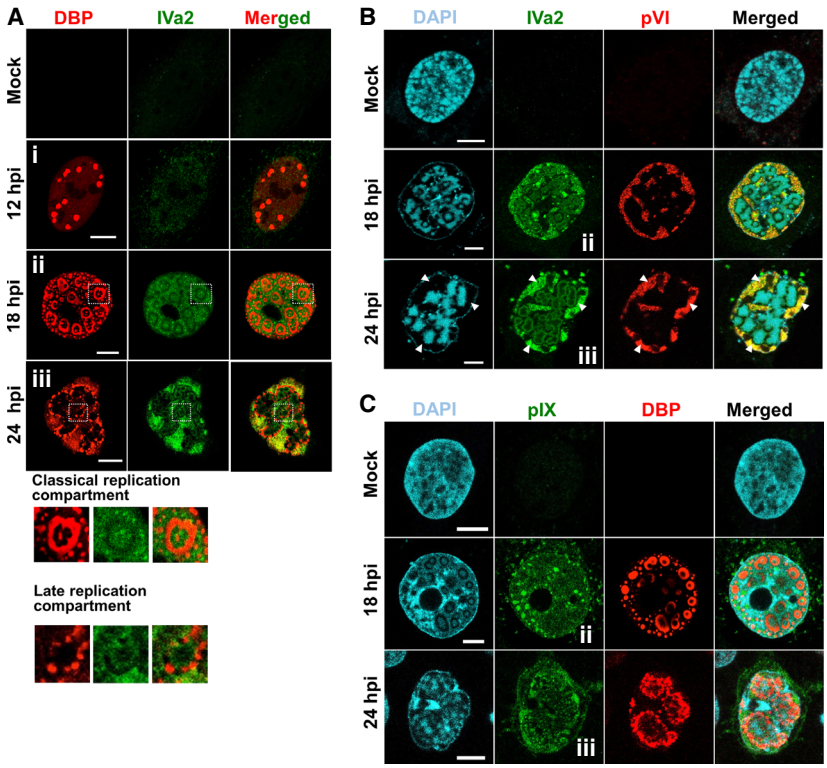

Fig. 2. Putative sites of Ad genome packaging and capsid assembly. U2OS cells were either mock infected or infected with HAdV5 and subjected to immunofluorescence analyses at 12, 18, and 24 hpi for A, 18 and 24 hpi for B and C using the antibodies against DBP and IVa2 (A), pVI and IVa2 (B), and DBP and pIX (C). The most prominent localization patterns at each time point (patterns i–iii) were picked up and shown. DAPI was used to stain DNA. Scale bars indicate 10 μm. Arrowheads shown in B indicate 'DNA-free region' where IVa2 and pVI are clearly colocalized (see the main text).

environment favorable for virus replication [33]. Both pVI and pIX were excluded from the ViPR body, suggesting that the ViPR body is not the site for Ad virion assembly. On the basis of the colocalization of capsid proteins and the viral genome-packaging protein, IVa2, virion assembly, including capsid assembly and genome packaging in late-stage Ad infection, occurs at the DNA-free regions outside the late replication compartments. IVa2 also accumulated in the periphery of the ViPR bodies suggesting additional functions.

Identification of ViPR body constituents

To address ViPR body's function, we identified factors accumulating in the ViPR body. First, we focused on NPM1. In a previous study, we demonstrated that localization of enhanced green fluorescent protein (EGFP)-tagged NPM1 does not clearly change during the Ad infection cycle; however, other studies have reported that localization of endogenous NPM1 changes upon Ad infection [27,34]. Indirect immunofluorescence assay with polyclonal antibody produced with the C-terminal half of NPM1 [35] clearly detected NPM1 in the nucleoli with weak staining of the nucleoplasm in mock-infected cells. NPM1 localization was unchanged and remained nucleolar in early stage Ad infection when DBP started to accumulate in the nucleus (pattern i cells) (Fig. 3A). However, we detected NPM1 colocalizing with viral DNA replication compartments in late-stage Ad infection in pattern ii cells. Notably, we found that NPM1 accumulated in the ViPR body in pattern iii cells (at 24 hpi). When NPM1 was costained with pVI, the two proteins showed a mutually exclusive localization pattern in late-stage Ad infection (Fig. 3B), suggesting that NPM1 plays a role in virus production before capsid assembly and genome packaging. We also examined the localization patterns of viral proteins and NPM1 in human alveolar basal epithelial cell line,

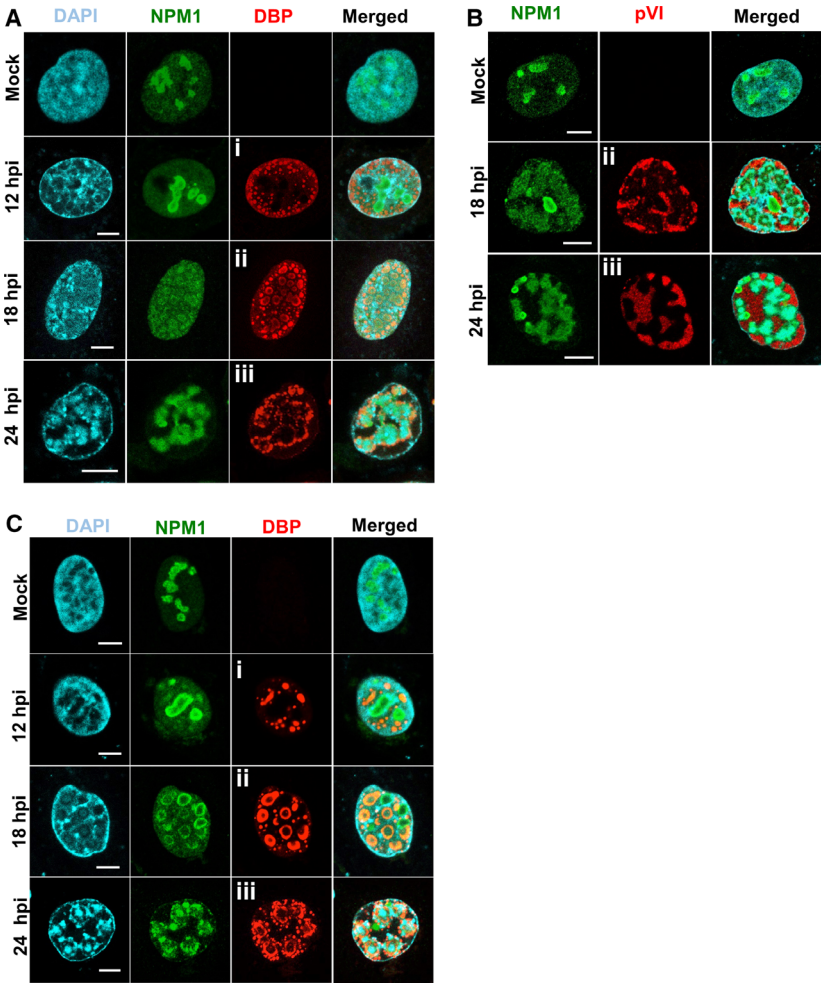

Fig. 3. NPM1 is recruited to the viral DNA replication sites and ViPR bodies in late-stage Ad infection. (A, B) U2OS cells were mock infected or infected with HAdV5 for 12, 18, and 24 h (A) or 18 and 24 h (B) and subjected to IF analyses with anti-NPM1 and anti-DBP (A) or anti-NPM1 and anti-pVI (B) antibodies. DAPI was used to stain DNA. Merged images are shown in the right column. (C) A549 cells were mock-infected or infected with HAdV5 for 12, 18, and 24 h and IF analyses with anti-NPM1 and anti-DBP were performed. DNA was stained with DAPI. Typical pattern i–iii cells determined from the localization patterns of DBP and DNA (A, C) were picked up at each time point and shown. Pattern ii and iii cells at 18 and 24 hpi, respectively, were picked up on the basis of DNA localization pattern in B. Scale bars indicate 10 μm.

A549 cells (Fig. 3C). Consistent with the data shown in U2OS cells, we observed that DBP showed mainly three distinct localization patterns in Ad-infected A549 cells and ViPR bodies were clearly formed in late-stage Ad infection based on DNA accumulation and disintegrated DBP rings (pattern iii cells). NPM1 was clearly colocalized with DBP rings in pattern ii cells and accumulated to ViPR bodies in pattern iii cells. We also noted that NPM1 was recruited to the DBP foci even in pattern i cells in A549 cells. It is likely that NPM1 was recruited to the DNA replication sites at early replication stage both in A549 and U2OS cells, but the amount of NPM1 at DBP foci in U2OS pattern i cells was very minor and undetectable.

In order to identify host factors involved in late-stage Ad infection, we examined the localization of NCL and UBF, two nucleolar chromatin regulatory proteins. We selected NCL and UBF because their localization patterns are reported to change upon Ad infection [27,28], although the exact localization patterns relative to ViPR bodies have not been tested previously. In mock-infected cells, UBF accumulated in the small foci inside the nucleoli, whereas NCL was detected mainly at the nucleolar periphery. We also found that at 24 hpi, both UBF and NCL (Fig. 4A,B) were colocalized with IVa2 at the periphery of the classical replication compartments in pattern ii cells. Because antibodies against NCL, UBF, and DBP were mouse monoclonal antibodies and we were unable to use at the same time to visualize NCL and UBF relative to DBP rings. However, classical replication compartments and ViPR bodies were easily found by DNA-staining patterns. In addition, when the ViPR body was formed, both UBF and NCL accumulated in the ViPR body marked by DNA staining. It should be noted that NCL was detected mainly at the edge of ViPR bodies with IVa2, whereas UBF was detected in the central region of these domains. These results demonstrated that various cellular chromatin regulatory proteins, including NPM1, UBF, and NCL, accumulated in the late replication compartments and the ViPR bodies possibly to remodel/reorganize the viral DNA/chromatin and/or to maintain the viral chromatin for its efficient encapsidation. Distinct localization patterns around the ViPR bodies of NPM1, UBF, and NCL suggested that these chromatin regulatory proteins play distinct roles at the periphery of or inside the ViPR bodies.

NPM1 regulation of ViPR body formation

In a previous study, we showed that NPM1 is required for virus production at a step downstream of Ad DNA replication and viral protein expression [22]. In addition, NPM1 depletion increases the association of core proteins with the viral genome [22]. Therefore, to test whether NPM1 plays an important role in the regulation of the nuclear organization of Ad-infected cells, we examined whether NPM1 depletion affects the formation of late replication compartments and the ViPR bodies. Control and NPM1-depleted U2OS cells infected with HAdV5 for 24 h were collected and subjected to western blotting (Fig. 5A). NPM1 depletion did not affect the expression level of several Ad proteins, as previously reported [22]. However, while the number of cells exhibiting pattern ii localization significantly increased, those showing pattern iii localization significantly decreased in number with NPM1

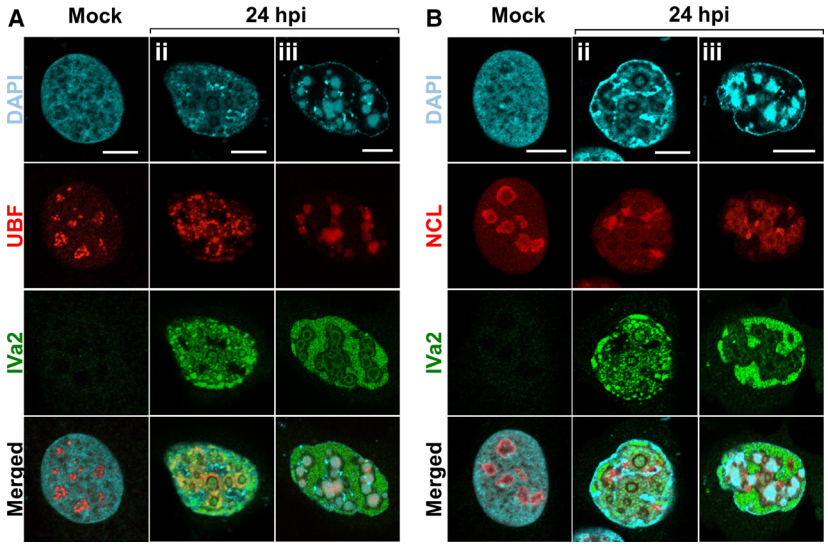

Fig. 4. UBF and NCL are components of Ad DNA replication compartments and ViPR body. At 24 hpi, mock- and HAdV5-infected U2OS cells were subjected to IF analyses with anti-IVa2 and anti-UBF (A) or anti-NCL (B) antibodies. Cells showing the localization patterns ii and iii based on DNA staining patters are shown. Scale bars indicate 10 μm.

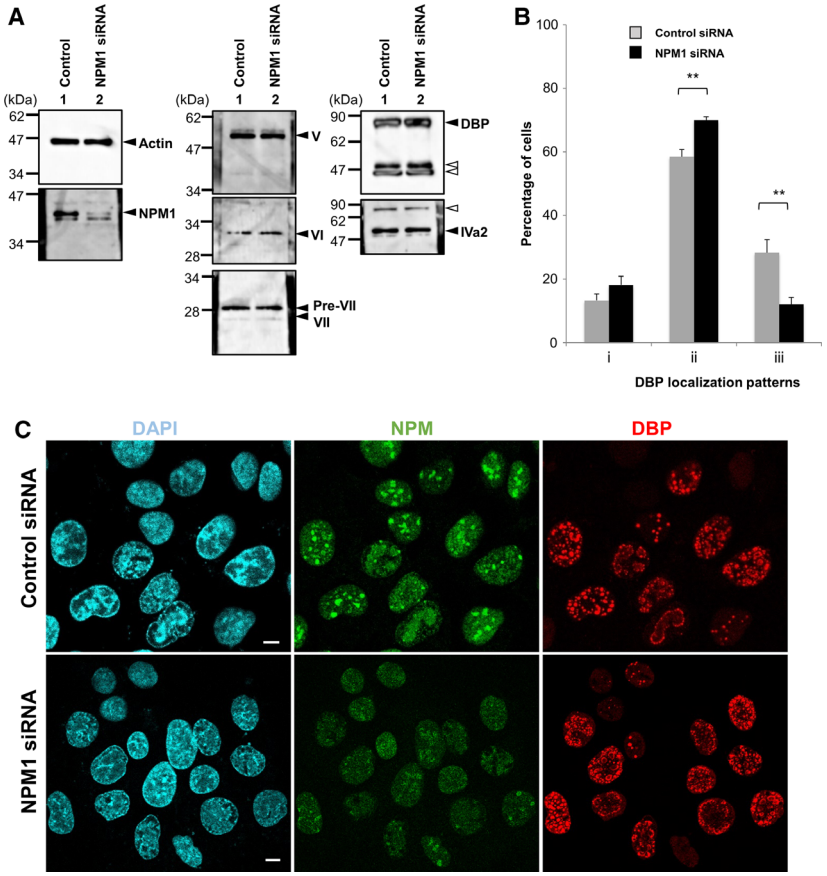

Fig. 5. NPM1 knockdown delayed the formation of ViPR body. (A) NPM1 knockdown did not affect adenoviral protein synthesis. Control and NPM1 siRNA-treated U2OS cells (lanes 1 and 2, respectively) were infected with HAdV5 (MOI = 20) at 60 h post siRNA transfection. At 24 hpi, cells were collected and the expression of Ad proteins, NPM1 and β-actin was examined by western blotting. Positions of molecular weight markers are shown at the left side of the panels. Positions of proteins are indicated by filled arrowheads. Antibodies for DBP and IVa2 detected additional proteins (blank arrowheads). (B, C) NPM1 depletion delayed the formation of the Ad late-replication compartments. Control and NPM-depleted cells as in A were infected with HAdV5, and at 24 hpi, cells were subjected to IF analysis with anti-DBP and anti-NPM1 antibodies and costained with DAPI to visualize DNA. In (B), cells exhibiting each DBP localization pattern were counted and the population of cells showing either pattern i to iii was graphed in percentage. Experiments were performed in triplicates and the number of cells counted were as follows: for control siRNA-treated cells, n = 125, 123, and 141; for NPM1 siRNA-treated cells, n = 158, 146, and 135. The average percentage of patterns i–iii are graphically represented in B, error bars indicate ±SD. P-values were calculated using student's t-test (**$P < 0.01$). Typical localization patterns for each siRNA-treated cell were shown in (C). Under our assay condition, most of cells showed low NPM1 expression when cells were treated with NPM1 siRNA. Scale bars indicate 10 μm.

depletion (Fig. 5B,C). These results suggested that NPM1 plays a critical role in the transition of the replication compartments from early to late ones and ViPR body formation.

In a previous study, using ChIP assay, we showed that core proteins V and VII and histone H3 on the virus genome increased due to NPM1 depletion [22]. Therefore, we hypothesized that replicated viral genomes were not properly packaged into viral chromatin in NPM1-depleted cells. To test this hypothesis, we examined micrococcal nuclease (MNase) sensitivity of viral DNA from control and NPM1-depleted cells infected with HAdV5. MNase preferentially digests DNA unbound with proteins and nucleosome repeats are visualized when cellular DNA is digested by MNase. When the Ad-infected cell nucleus is subjected to MNase digestion, viral genomic DNA is protected from MNase digestion, although clear repeating units of nucleosomes are not observed [36,37]. This suggests that replicated viral genomic DNA is packaged into virus-specific chromatin-like structure with core proteins. In addition, MNase digestion assay allows us to evaluate the amounts of proteins on DNA. Total DNAs from control and NPM1-depleted cells were

similarly digested by MNase (Fig. 6A). The amounts of viral genomic DNA and host *rRNA* gene (rDNA) after MNase digestion were analyzed by qPCR using primer sets specific for the *VA RNA* and *E1A* regions. We found that the amounts of amplified *VA RNA* and *E1A* gene products were significantly higher in NPM1-depleted cells compared to control siRNA-treated cells, whereas the amount of rDNA was not significantly changed, indicating that the viral genome forms a nuclease-resistant structure with NPM1 depletion (Fig. 6B).

We performed rescue experiments to confirm the effects of NPM1 depletion on the nuclease sensitivity of the viral genome. We used 293T cells because this cell line shows high transfection efficiency. We first examined whether ViPR bodies are formed in late-stage Ad infection in 293T cells as in U2OS cells by immunofluorescence analysis with anti-DBP and anti-NPM1 antibodies (Fig. 6C). The staining patterns of DBP and DNA in 293T cells were very similar to those in U2OS cells and three distinct localization patterns were detected. DNA accumulation sites in disintegrated DBP rings, which corresponded to ViPR bodies, were detected in pattern iii cells. In addition, NPM1 colocalization with DBP in pattern ii cells and with DNA (ViPR bodies) in pattern iii cells was also detected in 293T cells. These results indicated that the structural change in the infected cell nucleus upon Ad infection similarly occurred in both in 293T and U2OS cells. Following siRNA treatment, the cells were transfected with plasmids for Flag-tagged NPM1, infected with HAdV5, and subjected to MNase digestion assay. The siRNA used here targeted the 3′-untranslated region of the *NPM1* gene and the exogenous *NPM1* gene was resistant to siRNA-mediated down-regulation. Western blotting showed that NPM1 was efficiently depleted in 293T cells (compare Fig. 6D, lanes 1 and 2) and transfection of the plasmid rescued the amount of depleted NPM1 (lane 4). Consistent with the results obtained with U2OS cells (Fig. 6B), qPCR results showed that the amounts of Ad gene products amplified from NPM1-depleted cells were significantly higher compared to control cells (Fig. 6E). Exogenous expression of NPM1 tended to counteract the decrease in sensitivity to MNase digestion caused by NPM1 depletion, although the results were not statistically significant. Variation in the data could be due to the transfection efficiency under our assay condition, which was not 100%, and the inconsistent amount of exogenous NPM1 in individual cells. These results implied that NPM1 plays a critical role in the regulation of the viral chromatin structure by restricting the association of proteins, such as core proteins, to the viral genome. Furthermore, viral genome remodeling/reorganization by host factors, including NPM1, might be intimately associated with the late replication compartment and ViPR body formation.

Discussion

In this study, we confirmed ViPR body formation in late-stage Ad infection in several different cell lines. Additionally, we demonstrated that the viral packaging protein IVa2, but not capsid proteins pVI and pIX accumulates in the ViPR body. Although the exact function of the ViPR body is currently unknown, we propose that the ViPR body is the site for maintaining the reorganized viral genome to be packaged into the capsid. The reasons are as follows: First, viral core proteins, but not cellular histones or capsid proteins, are accumulated [13,29]. Second, cellular chromatin regulatory proteins, including NPM1, NCL, and UBF, are also accumulated (Figs 3 and 4), suggesting that they help maintain the viral chromatin structure. Finally, ViPR body formation is impaired by NPM1 depletion (Fig. 5). When NPM1 is depleted, the viral genome is bound by excess core proteins and fails to be reorganized/remodeled. NPM1-mediated viral chromatin remodeling at the late replication compartments is likely to be required for the accumulation of the Ad genome in the ViPR body.

With increasing the amounts of viral DNA in late-stage Ad infection, viral DNA accumulates and forms the ViPR body. Furthermore, when ViPR body formation is impaired by NPM1 depletion, virus production decreases [22], indicating that ViPR body formation is likely required for efficient virion production. Recent studies have shown that membrane-less structures are formed by liquid–liquid phase separation (LLPS) [38,39]. NPM1 induces LLPS by interacting with arginine-rich basic proteins and RNA. Given that core protein VII, an arginine-rich protein, accumulates in the ViPR body [13,29], NPM1 presumably plays a critical role in ViPR body formation by inducing phase separation via interaction with core proteins. Delayed ViPR body formation by NPM1 depletion might be explained, at least in part, by the ability of NPM1 to induce LLPS.

In addition to NPM1, nucleolar proteins UBF and NCL are also recruited to viral DNA replication compartments and ViPR bodies, suggesting their cooperative role in regulating viral chromatin remodeling and maintenance. Previous studies have reported that UBF is recruited to Ad replication sites, where it enhances viral DNA replication initiation [28]. From the localization in the late replication compartments and the

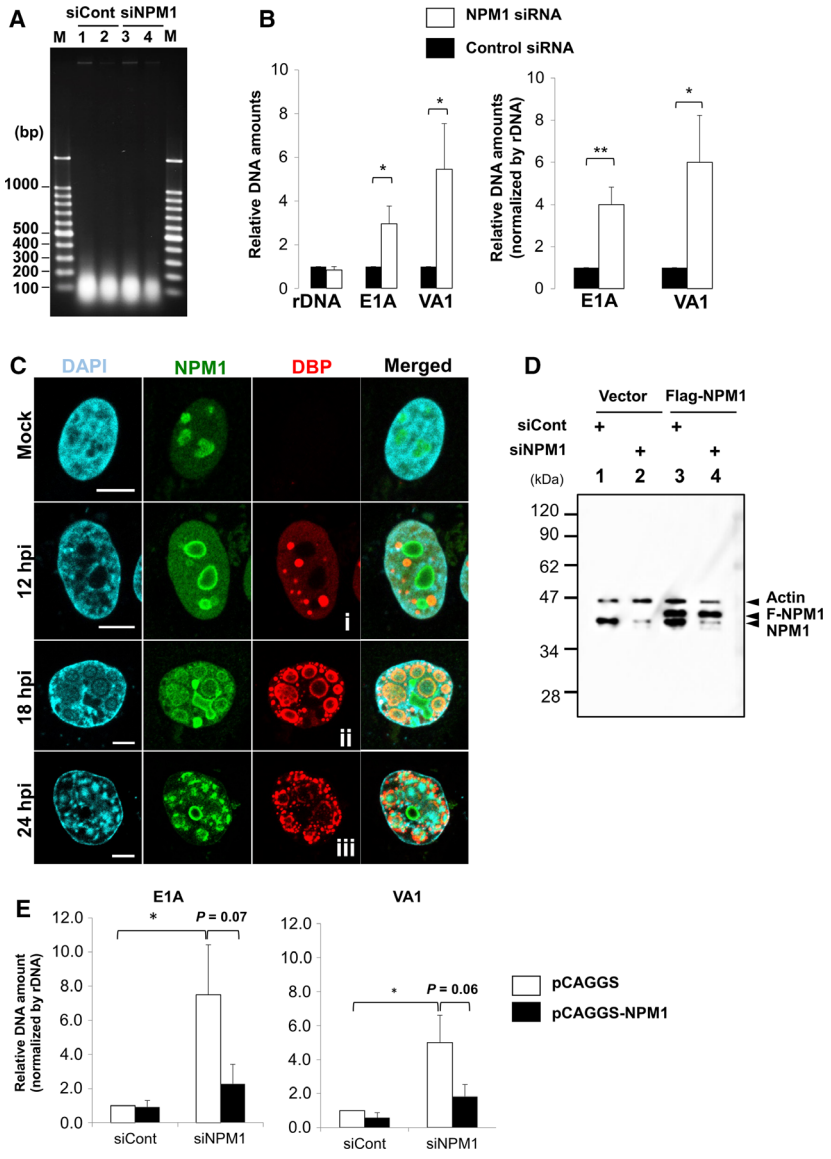

Fig. 6. NPM1 depletion decreased the sensitivity of adenoviral genome to nuclease digestion. U2OS cells treated with control or NPM1 siRNA were infected with HAdV5 (MOI = 20) 60 h post-siRNA transfection. At 24 hpi, the cells were digested with micrococcal nuclease and total DNA was extracted. (A) The purified genomic DNA was subjected to 1.6% agarose gel electrophoresis and visualized with GelRed staining. The DNAs for lanes 1 and 3, and 2 and 4 are control and NPM1 siRNA-treated cells, respectively. Lanes 1 and 2, and 3 and 4 represent two independent experiments. (B) Quantitative analyses of genomic DNA treated with MNase. The genomic DNA purified as in (A) were used as templates for qPCR with primer sets specific for rDNA, VA RNA, and E1A regions. The amounts of each DNA fragment in control siRNA-treated cells were set to 1.0 and relative amounts of DNAs from NPM1 siRNA-treated cells were calculated (left graph). The relative amounts of Ad DNA were normalized to that of rDNA and shown in right graph. Blank and filled bars indicate the DNA amounts from control cells and NPM1 siRNA-treated cells, respectively. (C) Immunofluorescence analysis of Ad-infected 293T cells. 293T cells were mock infected or infected with HAdV5 for 12, 18, and 24 h and subjected to IF analyses with anti-NPM1 and anti-DBP antibodies. DAPI was used to stain DNA. Patterns i–iii cells were picked up from samples of 12, 18, and 24 hpi. Scale bars indicate 10 μm. (D, E) Rescue experiments. Control and NPM1 siRNA-treated 293T cells were transfected with empty vector or pCAGGS-Flag-NPM1 at 36 h post siRNA transfection. Expression of NPM1 and β-actin was examined by Western blotting (D). Positions of actin, Flag-tagged NPM1 (F-NPM1), and NPM1 are shown at the left side of the panel. The infected cells were treated with MNase and the amounts of viral DNA were examined by qPCR as in (B). The data were average of three independent experiments and error bars are ±SD. The data were statistically analyzed by student's *t*-test (**P* < 0.05).

ViPR bodies, UBF might play a role in viral chromatin remodeling and maintenance, in addition to its role in DNA replication. On the other hand, although relocation of NCL to the cytoplasm by core protein V has been reported [27], the function and colocalization of NCL to viral replication compartments and the ViPR body have never been described. Since NCL and NPM1 share overlapping functions as histone chaperones [17,40], they might cooperatively regulate Ad genome replication and reorganization/remodeling in the late replication compartments. It should be also mentioned that NCL was detected at the periphery of the ViPR bodies, whereas NPM1 and UBF were detected inside the ViPR bodies. These results suggested that these proteins play distinct roles in the regulation of viral chromatin structure. To understand the molecular mechanism of viral genome reorganization prior to encapsidation in late-stage Ad infection, it is critical to determine the ViPR body constituents and their functions.

In summary, we proposed a model for viral chromatin remodeling and ViPR body formation (Fig. 7). Two distinct subnuclear structures in late-stage Ad infection are formed. Classical replication compartments are first formed, and then the structure is transformed to late replication compartments, possibly through an increase in the viral genome and core proteins. The viral genome replicated at the late replication compartments associates with viral core proteins quickly after synthesis and the amounts of core proteins on the viral genome are rigorously controlled by NPM1 to form proper viral chromatin structure. The properly assembled viral chromatin accumulates in the ViPR bodies. This viral chromatin remodeling step is possibly a prerequisite for ViPR body formation. LLPS mediated by the interaction between NPM1 and viral core proteins (viral chromatin) might play a crucial role in forming the ViPR body. In the ViPR body, the structure of the viral chromatin is maintained by host chromatin regulatory proteins such as NPM1 and UBF. Additional chromatin regulatory proteins including NCL might play roles in viral chromatin remodeling and maintenance in the late replication compartments and the ViPR bodies. The properly formed viral chromatin is sequentially transported to the sites of capsid assembly and genome packaging by an unknown mechanism.

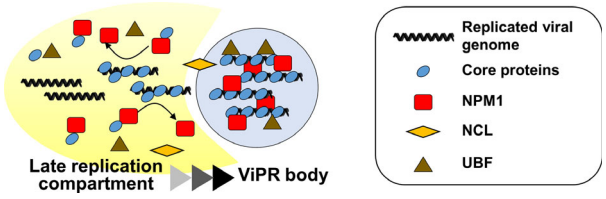

Fig. 7. Proposed model for Ad chromatin remodeling and ViPR body formation in late-stage Ad infection by host chromatin regulatory factors. The sites of the late replication compartment and the ViPR body are shown in yellow and blue, respectively. Upon viral DNA synthesis, core proteins are deposited on DNA to form viral chromatin structure. NPM1 mediates viral chromatin assembly in the late replication compartments. The properly assembled viral chromatin is accumulated in the ViPR body where the viral chromatin structure is maintained by NPM1 and UBF. NCL is mainly localized at the periphery of the ViPR bodies. The ViPR body formation might be mediated by LLPS by the host and viral proteins and DNA. When capsid proteins are accumulated outside the late replication compartments, the viral chromatin is transported to the sites for virion assembly.

Materials and methods

Cell culture and viruses

U2OS, A549, and 293T cells were maintained in Dulbecco's modified Eagle's medium (DMEM; Nissui, Nissui Pharmaceutical, Tokyo, Japan) containing heat-inactivated 10% FBS. Human adenovirus type 5 (HAdV5) used in this study was amplified and purified as described previously [26]. Cells to be infected were plated in culture dishes 1 day prior to infection and maintained in DMEM containing 10% FBS. Cells were infected with HAdV5 in DMEM without FBS for 1 h at multiplicity of infection (MOI) of 10–20. After washing with DMEM without FBS, cells were cultured at 37 °C in DMEM containing 5% FBS.

Antibodies

Polyclonal antibody recognizing NPM1 was previously described [35], monoclonal antibody for DBP was obtained from W. C. Russell (University of St Andrews, Fife, UK), antibodies against β-actin (C4), upstream binding factor (UBF) (F-9), NCL (D-6) were commercially available (Santa Cruz Biotechnology, Dallas, TX, USA). Antibody for pVI was previously described [41]. Antibodies for pV, pVII, pIX, and IVa2 were generated in rabbits using recombinant proteins.

Indirect immunofluorescence assay

Indirect immunofluorescence assays were performed essentially as described previously [26]. Briefly, cells grown on 15-mm coverslips (Matsunami, Matsunami Glass, Osaka, Japan) were fixed with 1.5% paraformaldehyde in PBS for 10 min at room temperature and then permeabilized with PBS containing 0.5% Triton X-100 for 20 min at room temperature. After blocking with 1% nonfat milk in PBS containing 0.1% Triton X-100 (PBS-T) for 15 min, samples

were incubated with primary antibodies. To detect the proteins, cells were incubated with secondary antibodies (AlexaFluor 488-conjugated anti-rabbit IgG, AlexaFluor 568-conjugated anti-mouse IgG; Thermo Fisher Scientific, Waltham, MA, USA) for 1 h in the dark. DNA was visualized by staining with DAPI for 15–30 min. Labeled cells were then observed by confocal laser-scanning microscopy (LSM700; Carl Zeiss, Oberkochen, Germany).

Quantitative analysis of viral DNA amounts by quantitative polymerase chain reaction

At 2, 8, 10, 12, and 14 h postinfection (hpi), Ad-infected U2OS cells (1×10^5) were collected and suspended in 10 mM tris pH7.9, 1 mM EDTA, and 0.1% Triton X-100. After incubating on ice for 5 min, the cells were collected, treated with proteinase K and RNase A at 50 °C for 1 h, and total DNA was isolated and purified by phenol/chloroform extraction and ethanol precipitation. The amount of Ad DNA was then examined by quantitative PCR (qPCR) with total DNA (10 ng) as a template and primer sets specific for the adenovirus *VA RNA* gene region (5′-GCT GGAGCAAAACCCAAATA-3′ and 5′-TATCTTGCGG G-CGTAAAACT-3′) and control for human *rRNA* gene (rDNA) (5′-TGACACGCTCACTGGCAGGCG-3′ and 5′-TGTGCGCAGGCGGCCTGGTG-3′). The amounts of viral DNA were normalized by that of rDNA.

NPM1 knock-down by siRNA

Stealth RNAi negative control and NPM1 RNAi (NPM1-HSS143154 Thermo Fisher Scientific, Waltham, MA, USA) were introduced into U2OS cells using Lipofectamine RNAiMAX (Thermo Fisher Scientific, Waltham, MA, USA) according to the manufacturer's protocol. To examine the effect of NPM1 knockdown on the localization of adenoviral proteins, control and NPM1 siRNA-treated U2OS cells at 60 h post-transfection were infected with HAdV5 at an MOI of 20. After 24 h, total U2OS cell lysates were prepared, and proteins were separated by SDS/PAGE and detected by western blotting. For rescue experiments, after siRNA transfection, plasmid DNA for the expression of Flag-tagged NPM1 (pCAGGS-Flag-NPM1 [42]) were transfected with Gene Juice (Novagen, Madison ,WI, USA).

MNase-qPCR experiment

U2OS cells treated with contol or NPM1 siRNA were grown in DMEM supplemented with 10% FBS at 37 °C and infected with HAdV5 (MOI = 20) at 60 h post-siRNA transfection. At 24 hpi, cells were suspended in 10× packed cell volume (PCV) of ice-cold reticulocyte standard buffer (RSB) [10 mM Tris-HCl (pH 7.9), 10 mM NaCl, 1.5 mM $MgCl_2$, 2 mM $CaCl_2$]. After 5 min of incubation on ice, the cells were centrifuged, resuspended in 10× PCV of ice-cold RSB containing 0.5% Triton X-100, incubated in ice for 10 min, washed with 10× PCV of RSB, resuspended in appropriate amount of RSB, and treated with micrococcal nuclease (MNase) (Roche Life Science, Merck KGaA, Darmstadt, Germany) (0.3 $U \cdot \mu L^{-1}$). The genomic DNA was isolated as above and was subjected to 1.6% agarose gel electrophoresis and stained with GelRed. In parallel, qPCR analysis was also conducted as mentioned above with a primer set specific for the Ad *VA RNA 1* gene region (see above), *E1A* promoter region (5′-GGG TCAAAGTTGGCGTTTTA-3′ and 5′-CAAAATGGCTA GGAGGTGGA-3′) and normalized using a primer set specific for rDNA (see above).

Acknowledgements

This work was supported by Grants-in-aid for Scientific Research from the Ministry of Education, Culture, Sports, Science and Technology of Japan to MO (26440021 and 17K07300) and TK (19H04838). HW is an INSERM fellow and received support through Equipe FRM DEQ20180339229. The authors would like to thank Enago (www.enago.jp) for the English language review.

Conflict of interest

The authors declare no conflict of interest.

Author contributions

MJG, KN, and MO designed the research; MJG and MH performed the research, MJG, TK, HW, KN, and MO analyzed data; and MJG, KN, HW, and MO wrote the paper. All authors reviewed the manuscript.

References

1 Lee CS, Bishop ES, Zhang R, Yu X, Farina EM, Yan S, Zhao C, Zheng Z, Shu Y, Wu X *et al.* (2017) Adenovirus-mediated gene delivery: potential applications for gene and cell-based therapies in the new era of personalized medicine. *Genes Dis* **4**, 43–63.
2 Chatterjee PK, Vayda ME & Flint SJ (1985) Interactions among the three adenovirus core proteins. *J Virol* **55**, 379–386.
3 Everitt E, Sundquist B, Pettersson U & Philipson L (1973) Structural proteins of adenoviruses. X. Isolation and topography of low molecular weight antigens from the virion of adenovirus type 2. *Virology* **52**, 130–147.
4 van Oostrum J & Burnett RM (1985) Molecular composition of the adenovirus type 2 virion. *J Virol* **56**, 439–448.
5 Nicolas JC, Young CS, Suarez F, Girard M & Levine AJ (1983) Detection, rescue, and mapping of mutations

in the adenovirus DNA binding protein gene. *Proc Natl Acad Sci USA* **80**, 1674–1677.
6 Roovers DJ, Young CS, Vos HL & Sussenbach JS (1990) Physical mapping of two temperature-sensitive adenovirus mutants affected in the DNA polymerase and DNA binding protein. *Virus Genes* **4**, 53–61.
7 Christensen JB, Byrd SA, Walker AK, Strahler JR, Andrews PC & Imperiale MJ (2008) Presence of the adenovirus IVa2 protein at a single vertex of the mature virion. *J Virol* **82**, 9086–9093.
8 Wohl BP & Hearing P (2008) Role for the L1-52/55K protein in the serotype specificity of adenovirus DNA packaging. *J Virol* **82**, 5089–5092.
9 Pérez-Berná AJ, Mangel WF, McGrath WJ, Graziano V, Flint J & San Martín C (2014) Processing of the l1 52/55k protein by the adenovirus protease: a new substrate and new insights into virion maturation. *J Virol* **88**, 1513–1524.
10 Ahi YS, Vemula SV, Hassan AO, Costakes G, Stauffacher C & Mittal SK (2015) Adenoviral L4 33K forms ring-like oligomers and stimulates ATPase activity of IVa2: implications in viral genome packaging. *Front Microbiol* **6**, 318.
11 Condezo GN, Marabini R, Ayora S, Carazo JM, Alba R, Chillón M & San Martín C (2015) Structures of adenovirus incomplete particles clarify capsid architecture and show maturation changes of packaging protein L1 52/55k. *J Virol* **89**, 9653–9664.
12 Wu K, Orozco D & Hearing P (2012) The adenovirus L4-22K protein is multifunctional and is an integral component of crucial aspects of infection. *J Virol* **86**, 10474–10483.
13 Komatsu T, Robinson DR, Hisaoka M, Ueshima S, Okuwaki M, Nagata K & Wodrich H (2016) Tracking adenovirus genomes identifies morphologically distinct late DNA replication compartments. *Traffic* **17**, 1168–1180.
14 Condezo GN & San Martín C (2017) Localization of adenovirus morphogenesis players, together with visualization of assembly intermediates and failed products, favor a model where assembly and packaging occur concurrently at the periphery of the replication center. *PLoS Pathog* **13**, e1006320.
15 Dumbar TS, Gentry GA & Olson MO (1989) Interaction of nucleolar phosphoprotein B23 with nucleic acids. *Biochemistry* **28**, 9495–9501.
16 Herrera JE, Savkur R & Olson MO (1995) The ribonuclease activity of nucleolar protein B23. *Nucleic Acids Res* **23**, 3974–3979.
17 Okuwaki M, Matsumoto K, Tsujimoto M & Nagata K (2001) Function of nucleophosmin/B23, a nucleolar acidic protein, as a histone chaperone. *FEBS Lett* **506**, 272–276.
18 Szebeni A & Olson MO (1999) Nucleolar protein B23 has molecular chaperone activities. *Protein Sci* **8**, 905–912.
19 Itahana K, Bhat KP, Jin A, Itahana Y, Hawke D, Kobayashi R & Zhang Y (2003) Tumor suppressor ARF degrades B23, a nucleolar protein involved in ribosome biogenesis and cell proliferation. *Mol Cell* **12**, 1151–1164.
20 Okuda M, Horn HF, Tarapore P, Tokuyama Y, Smulian AG, Chan PK, Knudsen ES, Hofmann IA, Snyder JD, Bove KE *et al.* (2000) Nucleophosmin/B23 is a target of CDK2/cyclin E in centrosome duplication. *Cell* **103**, 127–140.
21 Samad MA, Okuwaki M, Haruki H & Nagata K (2007) Physical and functional interaction between a nucleolar protein nucleophosmin/B23 and adenovirus basic core proteins. *FEBS Lett* **581**, 3283–3288.
22 Samad MA, Komatsu T, Okuwaki M & Nagata K (2012) B23/nucleophosmin is involved in regulation of adenovirus chromatin structure at late infection stages, but not in virus replication and transcription. *J Gen Virol* **93**, 1328–1338.
23 Ugai H, Dobbins GC, Wang M, Le LP, Matthews DA & Curiel DT (2012) Adenoviral protein V promotes a process of viral assembly through nucleophosmin 1. *Virology* **432**, 283–295.
24 Jeong H, Cho MH, Park SG & Jung G (2014) Interaction between nucleophosmin and HBV core protein increases HBV capsid assembly. *FEBS Lett* **588**, 851–858.
25 Day PM, Thompson CD, Pang YY, Lowy DR & Schiller JT (2015) Involvement of nucleophosmin (NPM1/B23) in assembly of infectious HPV16 capsids. *Papillomavirus Res* **1**, 74–89.
26 Haruki H, Okuwaki M, Miyagishi M, Taira K & Nagata K (2006) Involvement of template-activating factor I/SET in transcription of adenovirus early genes as a positive-acting factor. *J Virol* **80**, 794–801.
27 Matthews DA (2001) Adenovirus protein V induces redistribution of nucleolin and B23 from nucleolus to cytoplasm. *J Virol* **75**, 1031–1038.
28 Lawrence FJ, McStay B & Matthews DA (2006) Nucleolar protein upstream binding factor is sequestered into adenovirus DNA replication centres during infection without affecting RNA polymerase I location or ablating rRNA synthesis. *J Cell Sci* **119**, 2621–2631.
29 Komatsu T, Quentin-Froignant C, Carlon-Andres I, Lagadec F, Rayne F, Ragues J, Kehlenbach RH, Zhang W, Ehrhardt A, Bystricky K *et al.* (2018) *In vivo* labelling of adenovirus DNA identifies chromatin anchoring and biphasic genome replication. *J Virol* **92**, e00795-18.
30 Pombo A, Ferreira J, Bridge E & Carmo-Fonseca M (1994) Adenovirus replication and transcription sites are spatially separated in the nucleus of infected cells. *EMBO J* **13**, 5075–5085.
31 Ostapchuk P, Yang J, Auffarth E & Hearing P (2005) Functional interaction of the adenovirus IVa2 protein

with adenovirus type 5 packaging sequences. *J Virol* **79**, 2831–2838.
32 Perez-Romero P, Tyler RE, Abend JR, Dus M & Imperiale MJ (2005) Analysis of the interaction of the adenovirus L1 52/55-kilodalton and IVa2 proteins with the packaging sequence in vivo and in vitro. *J Virol* **79**, 2366–2374.
33 Parks RJ (2005) Adenovirus protein IX: a new look at an old protein. *Mol Ther* **11**, 19–25.
34 Hindley CE, Davidson AD & Matthews DA (2007) Relationship between adenovirus DNA replication proteins and nucleolar proteins B23.1 and B23.2. *J Gen Virol* **88**, 3244–3248.
35 Hisaoka M, Nagata K & Okuwaki M (2014) Intrinsically disordered regions of nucleophosmin/B23 regulate its RNA binding activity through their inter- and intra-molecular association. *Nucleic Acids Res* **42**, 1180–1195.
36 Daniell E, Groff DE & Fedor MJ (1981) Adenovirus chromatin structure at different stages of infection. *Mol Cell Biol* **1**, 1094–1105.
37 Déry CV, Toth M, Brown M, Horvath J, Allaire S & Weber JM (1985) The structure of adenovirus chromatin in infected cells. *J Gen Virol* **66** (Pt 12), 2671–2684.
38 Mitrea DM, Cika JA, Guy CS, Ban D, Banerjee PR, Stanley CB, Nourse A, Deniz AA & Kriwacki RW (2016) Nucleophosmin integrates within the nucleolus via multi-modal interactions with proteins displaying R-rich linear motifs and rRNA. *Elife* **5**,e13571.
39 Mitrea DM, Cika JA, Stanley CB, Nourse A, Onuchic PL, Banerjee PR, Phillips AH, Park CG, Deniz AA & Kriwacki RW (2018) Self-interaction of NPM1 modulates multiple mechanisms of liquid-liquid phase separation. *Nat Commun* **9**, 842.
40 Angelov D, Bondarenko VA, Almagro S, Menoni H, Mongélard F, Hans F, Mietton F, Studitsky VM, Hamiche A, Dimitrov S *et al*. (2006) Nucleolin is a histone chaperone with FACT-like activity and assists remodeling of nucleosomes. *EMBO J* **25**, 1669–1679.
41 Martinez R, Schellenberger P, Vasishtan D, Aknin C, Austin S, Dacheux D, Rayne F, Siebert A, Ruzsics Z, Gruenewald K *et al*. (2015) The amphipathic helix of adenovirus capsid protein VI contributes to penton release and postentry sorting. *J Virol* **89**, 2121–2135.
42 Okuwaki M, Tsujimoto M & Nagata K (2002) The RNA binding activity of a ribosome biogenesis factor, nucleophosmin/B23, is modulated by phosphorylation with a cell cycle-dependent kinase and by association with its subtype. *Mol Biol Cell* **13**, 2016–2030.